JOURNAL OF CATALYSIS **110**, 330–347 (1988)

Characterization and Catalytic Studies of Y-Zeolites Coexchanged with Iron and a Second Polyvalent Cation

LUIS M. APARICIO,* MARIA A. ULLA,† W. S. MILLMAN,† AND J. A. DUMESIC*,[1]

*Department of Chemical Engineering, University of Wisconsin, Madison, Wisconsin 53706; and
†Department of Chemistry, University of Wisconsin, Milwaukee, Wisconsin 53201*

Received July 22, 1987; revised October 14, 1987

Y-zeolites exchanged with both Fe and either Ca, La, Eu, Cr, Mn, Co, Ni, or Cu were characterized by magnetic susceptibility measurements and Mössbauer spectroscopy. In addition, these zeolites were studied as catalysts for the oxidation of CO with NO and for the decomposition of N_2O into N_2 and O_2. The results showed that Ca, La, and Eu cations in FeCa–Y, FeLa–Y, and FeEu–Y occupy primarily site I, forcing a large fraction of Fe cations to sites I′, II, and/or II′. Such zeolites exhibited higher reaction rates than Fe–Y for both reactions. Coexchanged, first-row transition metals had a different effect on the Fe. For example, Mn, Ni, and Cu cations in FeMn–Y, FeNi–Y, and FeCu–Y were found to make the Fe more oxidizable and less reducible. Reaction rates measured over Cr–Y, Mn–Y, Fe–Y, Co–Y, Ni–Y, and Cu–Y showed that the oxidizability of these cations decreases in the order Cr(III) > Fe(II), Cu(I) > Co(II) > Mn(II), Ni(II). Finally, the Fe in FeEu–Y was found to enhance the reducibility of the Eu. © 1988 Academic Press, Inc.

INTRODUCTION

The ability of zeolites exchanged with iron, copper, and chromium to act as redox catalysts has been documented in the literature in recent years (*1–6*). Redox reactions are believed to occur over these zeolites via a mechanism involving separate oxidation and reduction steps. According to the proposed mechanism, oxidizing gases like O_2, NO, and N_2O react with Fe(II), Cu(I), Cr(II), or Cr(III) cations in the zeolites, oxidizing them and depositing extralattice oxygen on the cations in the process. In a second step, gases such as H_2, CO, or N_2O extract the extralattice oxygen, reducing the cations and producing either H_2O, CO_2, or N_2, and O_2. Although the zeolites studied so far have exhibited the same general behavior, some differences between them have been discovered. For example, Fe–Y zeolite is more active for the oxidation of Co when O_2 rather than N_2O is the oxidizing agent. In contrast, Fe–mordenite is more active for the same reaction when N_2O rather than O_2 is the oxidizing agent (*2*). In addition, Fe–mordenite has higher turnover frequencies than Fe–Y for the oxidation of CO with various oxidizing agents and for the decomposition of N_2O into its elements (*2, 5*). Cu–Y also differs somewhat from Fe–Y. When CO is oxidized with excess O_2 over Fe–Y, the rate law is first order in CO (*2*). Under the same conditions, the rate law can be zero order in CO when Cu–Y is the catalyst (*3*).

In an effort to explain such differences in behavior between various zeolites, work in our laboratories has concentrated on the identification of factors that can affect the activities of transition metal-exchanged zeolites for redox reactions. In a recent paper, we reported the results of an investigation of the effect of the Si/Al ratio on the catalytic properties of Fe–Y. It was found that Fe–Y zeolites with Si/Al ratios of 4 to 9 had a larger fraction of iron cations in sites I′, II, and/II′ than conventional Fe–Y, which has a Si/Al ratio of 2.5. The samples with higher Si/Al ratios were also found to

---

[1] To whom correspondence should be addressed.

0021-9517/88 $3.00

have higher turnover frequencies than conventional Fe–Y for the decomposition of N_2O (*6*). In another paper, we reported the effects the zeolite lattice can have on the species that form upon adsorption of NO on iron zeolites. It was found that zeolites with iron cations in more accessible sites favor the formation of mononitrosyl over dinitrosyl species (*7*). In this paper, we report results of an investigation of another factor that can influence the catalytic properties of iron zeolites, namely the presence of coexchanged polyvalent cations.

In the work described here, we have studied whether coexchanged polyvalent cations can alter either the site locations of exchanged iron cations or their ability to undergo oxidation and reduction. The coexchanged Y-zeolites prepared for this investigation were FeCa–Y, FeLa–Y, FeEu–Y, FeCr–Y, FeMn–Y, FeCo–Y, FeNi–Y, and FeCu–Y. These zeolites were prepared by sequential exchange, adding the noniron cations first, and then exchanging with iron. Calcium, lanthanum, and europium were chosen because of their large cationic radii. Large polyvalent cations are believed to have a strong preference for site I because at that site they are bonded to six oxygen atoms that can balance the cationic charge and because the cation–oxygen bond length is relatively long (ca. 0.27 nm). These cations can therefore be expected to change the distribution of coexchanged Fe cations among the exchange sites. The other five cations were chosen to study the effect of first-row transition metal cations on coexchanged iron.

The location of the iron cations in these zeolites was studied by ^{57}Fe Mössbauer spectroscopy. This technique can differentiate between iron cations in sites of low coordination (sites I′, II, and/or II′) and sites of high coordination (site I) (*6*). The relative oxidizabilities and reducibilities of the exchanged cations were determined by measuring the rates of two redox reactions over the zeolites. For one of these reactions, the oxidation of CO with NO, the rate-determining step over Fe–Y is believed to be the oxidation of Fe(II) to Fe(III) by NO (*2*). For the other reaction, the decomposition of N_2O into its elements, the rate-determining step is believed to be the reduction of Fe(III) by N_2O (*4*). Thus, the rates of these two reactions over the samples provided a qualitative measure of the oxidizabilities and reducibilities of the cations.

For comparison with results obtained for the coexchanged zeolites, the rates of these two reactions were also measured over Y-zeolites exchanged with only the second cation (but not iron). In addition, the oxidation states after oxidation and reduction treatments were studied for Cr–Y, Mn–Y, Fe–Y, Co–Y, Ni–Y, and Cu–Y by measuring the paramagnetic susceptibilities of these zeolites. The oxidation state of Eu in Eu–Y and FeEu–Y was monitored after oxidation and reduction treatments using ^{151}Eu Mössbauer spectroscopy.

EXPERIMENTAL

The starting material for all the samples of this study was Linde Na–Y (SK-40, lot 1280-133). Before ion exchange, the Na–Y zeolite was washed with a pH 5.0 buffer solution. Samples were prepared by contacting this Na–Y with solutions of $CaCl_2$ (1.0 *M*), $La(NO_3)_3$ (0.5 *M*), $EuCl_3$ (0.1 *M*), $Cr(NO_3)_3$ (0.2 *M*), $Mn(NO_3)_2$ (0.1 *M*), $Co(NO_3)_2$ (0.2 *M*), $Ni(NO_3)_2$ (0.5 *M*), and $Cu(NO_3)_2$ (0.2 *M*) at 360 K for 3 days. Before contact with Na–Y, dilute NaOH was added to the Cr, Mn, Co, Ni, and Cu nitrate solutions to adjust the pH to 4.0. After ion exchange, the zeolites were washed with distilled water and dried in air at 400 K for ca. 5 h. The coexchanged zeolites were prepared by contacting these samples with an $FeSO_4$ solution in a nitrogen atmosphere. The pH during this procedure was maintained at 3.9 ± 0.2. After exchange with iron, the samples were washed with a dilute H_2SO_4 solution of pH 4.0, dried in N_2 at 400 K for ca. 5 h, and finally oxidized with O_2, starting at 370 K, and increasing the tem-

TABLE 1

Unit Cell Compositions

Fe–Y[a]:	$(SiO_2)_{137}(AlO_2)_{55}Na_{22.6}Fe_{13.6}H_{4.40}$
Ca–Y:	$(SiO_2)_{137}(AlO_2)_{42}Na_{6.7}Ca_{21}$
La–Y:	$(SiO_2)_{137}(AlO_2)_{49}Na_{12}La_{14}$
Eu–Y:	$(SiO_2)_{137}(AlO_2)_{49}Na_{12}Eu_{13}$
Cr–Y:	$(SiO_2)_{137}(AlO_2)_{40}Na_{9.0}Cr_{17}$
Mn–Y:	$(SiO_2)_{137}(AlO_2)_{55}Na_{15}Mn_{20}$
Co–Y:	$(SiO_2)_{137}(AlO_2)_{53}Na_{13}Co_{17}H_{6.0}$
Ni–Y:	$(SiO_2)_{137}(AlO_2)_{54}Na_{13}Ni_{17}H_{7.0}$
Cu–Y:	$(SiO_2)_{137}(AlO_2)_{54}Na_{12}Cu_{20}H_{2.0}$
FeCa–Y:	$(SiO_2)_{137}(AlO_2)_{43}Na_{7.2}Fe_{7.5}Ca_{14}$
FeLa–Y:	$(SiO_2)_{137}(AlO_2)_{49}Na_{7.5}Fe_{6.6}La_{10}$
FeEu–Y:	$(SiO_2)_{137}(AlO_2)_{51}Na_{8.7}Fe_{10}Eu_{7.7}$
FeCr–Y:	$(SiO_2)_{137}(AlO_2)_{39}Na_{8.9}Fe_{8.9}Cr_{18}$
FeMn–Y:	$(SiO_2)_{137}(AlO_2)_{52}Na_{12}Fe_{13}Mn_{6.4}H_{1.2}$
FeCo–Y:	$(SiO_2)_{137}(AlO_2)_{52}Na_{11}Fe_{15}Co_{3.4}H_{4.2}$
FeNi–Y:	$(SiO_2)_{137}(AlO_2)_{53}Na_{13}Fe_{14}Ni_{4.7}H_{2.6}$
FeCu–Y:	$(SiO_2)_{137}(AlO_2)_{56}Na_{12}Fe_{13}Cu_{8.3}H_{1.4}$

[a] The chemical composition of the Fe–Y sample was determined by Galbraith laboratories.

perature by 50 K every 30 min until reaching 620 K. The unit cell compositions of the resulting zeolites, obtained with a Beckman Spectraspan IV plasma spectrophotometer, are summarized in Table 1.

The retention of the crystallinity after these exchanges was checked qualitatively by collecting powder X-ray diffraction patterns for all the samples. These diffraction patterns are shown in Fig. 1. All the exchanged zeolites displayed the same peaks as those of Na–Y, although the relative intensities of these varied somewhat. In general, all samples gave peaks that were as strong as those of Na–Y; hence, no substantial loss of crystallinity was detected by X-ray diffraction. However, the unit cell compositions given in Table 1 show that some dealumination occurred during exchange with Ca, La, Eu, and Cr. The zeolites in which dealumination was most extensive were Cr–Y and FeCr–Y. A further peculiarity of the Cr–Y and FeCr–Y zeolites was that their unit cell compositions showed that they apparently have cations in excess of their exchange capacity (see Table 1). A possible explanation for this is that Cr(III) ions partially dealuminated these zeolites, but "healed" the structure by replacing Al atoms in the lattice. This behavior of Cr(III) cations has been reported previously (*8*). These complications could have been avoided with lower exchange levels, but high levels of exchange were needed to study the influence of chromium cations on coexchanged iron.

Mössbauer spectra were collected using an Austin Science Associates Model S-600 Mössbauer spectrometer controller and a Tracor-Northern Model N6-900 multichannel analyzer. The details of the ^{57}Fe Mössbauer spectroscopy experiments have been outlined elsewhere (*6*). For the ^{151}Eu spectra, a 50-mCi source of $^{151}SmF_3$ was used. The velocity scale of the spectrometer was calibrated by collecting spectra of EuS_2 and

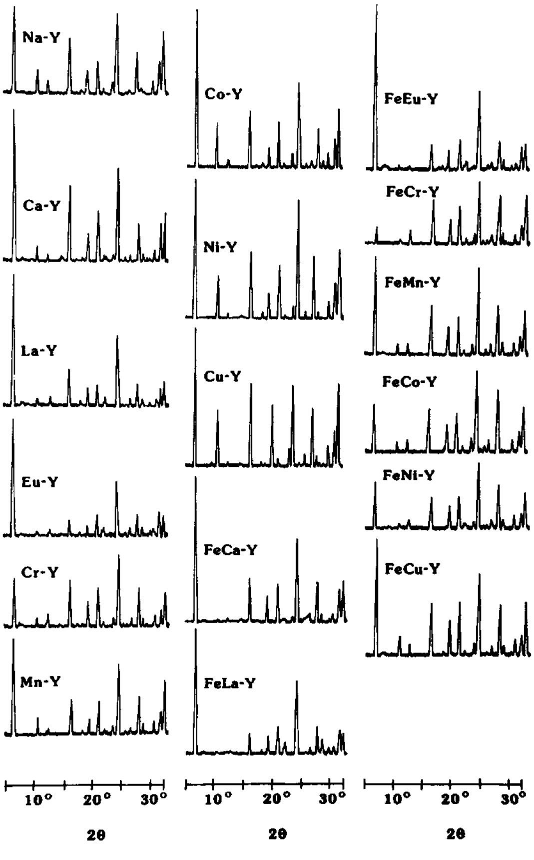

FIG. 1. X-ray diffraction patterns.

EuF_3. All europium isomer shifts are reported relative to EuF_3, while iron isomer shifts are reported relative to metallic Fe. Before the spectra were collected, the samples were treated in either flowing O_2 or flowing H_2 (ca. 150 cm^3/min) at 700 K for 5 h. The O_2 treatment oxidizes all the iron to Fe(III), while the H_2 treatment reduces all the iron to Fe(II).

Reaction rates were measured with a single-pass flow microreactor operating at near-atmospheric pressure. For the oxidation of CO with NO, the inlet gas contained 3% CO and 6% NO by volume, the balance being He. For the N_2O decomposition reaction, the inlet gas contained 8% N_2O, the balance being He. The catalyst weight on a dry basis was 1.0 g in all experiments. The total flow rate of the inlet stream was 200 cm^3/min for all runs. The CO stream was purified by passage through a 13X molecular sieve trap at 200 K, the NO stream by passage through a glass bead trap at 200 K, the N_2O stream by passage through a 13X molecular sieve trap at room temperature, and the He stream by passage through a molecular sieve trap at 78 K. The effluent was analyzed with a gas chromatograph operating with a Porapak QS column. For the reaction of CO with NO, the column was operated at 200 K until N_2, CO, and NO were eluted, and the temperature was then raised to 300 K for the elution of CO_2 and any N_2O present. For the decomposition of N_2O, the column was operated at 270 K. Before these experiments, the zeolites were pretreated with O_2 at 700 K for ca. 4 h.

With two exceptions (the reduction of NO by CO over Cr–Y and FeCr–Y), the turnover frequencies of this study were sufficiently low that diffusional limitations can be neglected. Specifically, the Thiele modulus can be estimated to be less than 0.1 for the kinetic measurements of this study, using the diffusivity and average particle diameter values given by Miró *et al.* (*9*).

Magnetic susceptibility measurements were carried out using the Faraday method with a Cahn Model 2000 electrobalance and an electromagnet capable of generating fields up to 6 kG. Before these measurements, the zeolites were either oxidized with flowing O_2 (ca. 150 cm^3/min) at 700 K for 3 h or reduced with flowing H_2 (ca. 150 cm^3/min) at 700 K for 3 h. The measurements were performed *in vacuo* at room temperature and at 200 K. The gases for the treatments were purified in the same way as that for the Mössbauer spectroscopy experiments. All samples exhibited both paramagnetic and superparamagnetic behavior. The superparamagnetism was present in the original Linde Na–Y, indicating that it arose from a ferromagnetic impurity in the original zeolite. Such ferromagnetic impurities in Linde zeolites have been reported previously (*10*). The data were therefore fit to paramagnetic and superparamagnetic contributions, and magnetic moments were calculated from the paramagnetic signal.

RESULTS

FeCa–Y, FeLa–Y, and FeEu–Y

Figure 2 shows ^{57}Fe Mössbauer spectra of FeCa–Y, FeLa–Y, and FeEu–Y after oxidation with O_2. The spectra are similar to those obtained previously for Fe–Y (*6, 11*), showing a broad Fe(III) doublet. Figure 3 shows spectra of the same zeolites collected after reduction with H_2. These spectra exhibit two Fe(II) doublets, one with a larger isomer shift and quadrupole splitting, denoted as the outer doublet. This doublet has been assigned to ferrous cations at site I. The other doublet, denoted as the inner doublet, has been assigned to ferrous cations at sites I′, II, and/or II′ (*12*). In conventional Fe–Y, the inner doublet comprises only 16% of the total spectra area. In contrast, the inner doublet in FeCa–Y, FeLa–Y, and FeEu–Y contributes 38, 57, and 64%, respectively, of the total spectral area. Thus, the spectra of Fig. 3 show that these zeolites have a larger fraction of iron cations in sites I′, II, and/or II′ than that of conventional Fe–Y.

Since the FeLa–Y and FeEu–Y samples had the highest fraction of iron cations in

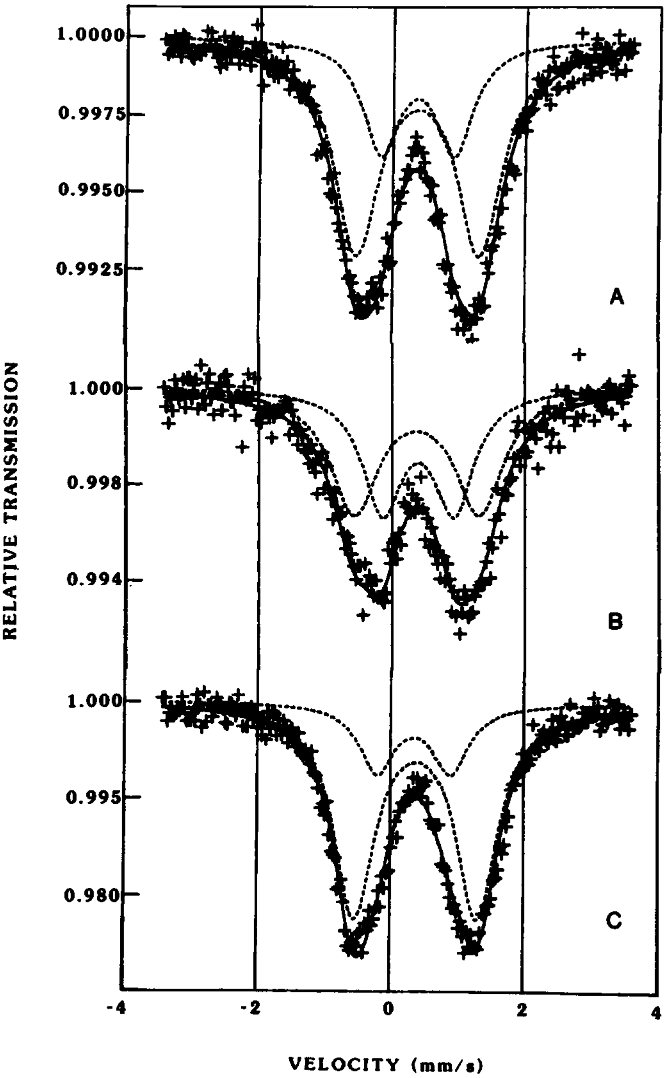

FIG. 2. Room temperature iron-57 Mössbauer spectra of (A) FeCa–Y, (B) FeLa–Y, and (C) FeEu–Y after oxidation pretreatment.

the sodalite unit and/or the supercage, their activities for both catalytic redox reactions were studied. The results are shown in Fig. 4. For comparison, results obtained under identical conditions for Fe–Y, La–Y, and Eu–Y are also shown. The figure demonstrates that although La–Y and Eu–Y show no measurable activity for the reactions, FeLa–Y and FeEu–Y have a higher activity for both reactions than Fe–Y. Hence, the reaction rate measurements are in agreement with the Mössbauer spectroscopy results, indicating that a larger fraction of iron in the more accessible sites leads to enhanced catalytic activity.

Figure 5 shows ^{151}Eu Mössbauer spectra of Eu–Y and FeEu–Y after oxidation with O_2 and reduction with H_2. The spectra of Eu–Y contain only one peak centered at ca. 0 mm/s, indicating that the oxidation state of Eu was Eu(III), even after treatment with H_2 at 700 K for 5 h. The europium in FeEu–Y behaves differently, with a Eu(II) peak centered at ca. −15 mm/s appearing

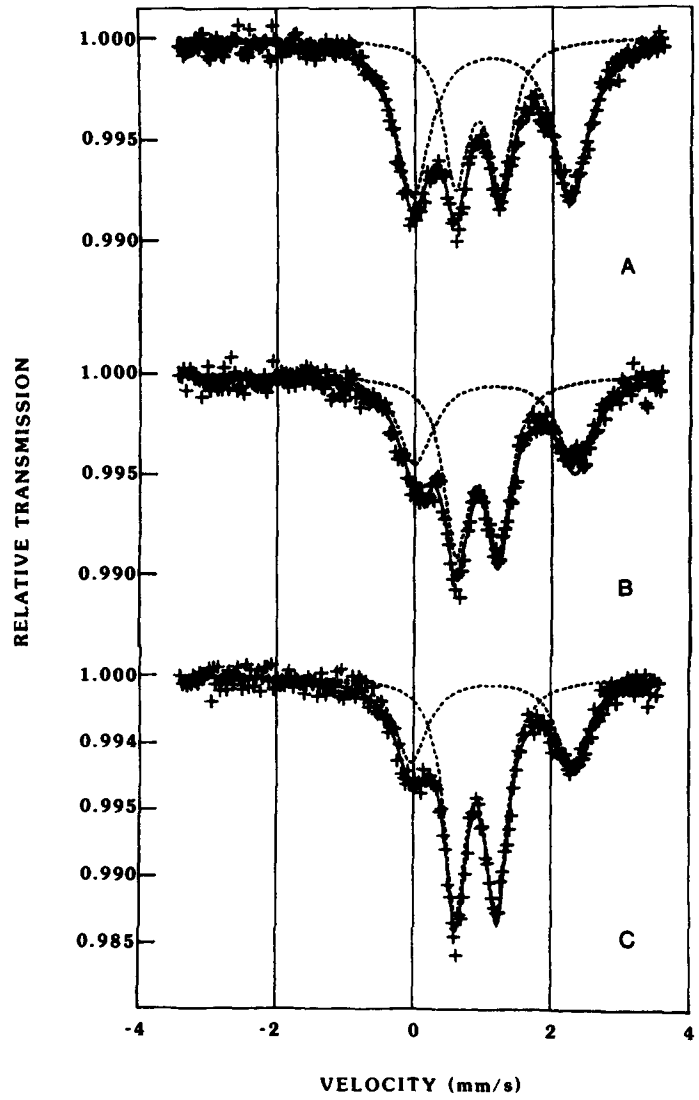

FIG. 3. Room temperature iron-57 Mössbauer spectra of (A) FeCa-Y, (B) FeLa-Y, and (C) FeEu-Y after reduction pretreatment.

after the H_2 pretreatment. The result shows that the presence of Fe in the zeolite facilitates the reduction of coexchanged Eu. The parameters obtained by computer-fitting the spectra of Figs. 2, 3, and 5 are summarized in Table 2.

Cr-Y, Mn-Y, Fe-Y, Co-Y, Ni-Y, and Cu-Y

Magnetic moments calculated for the exchange cations from their paramagnetic susceptibilities are listed in Table 3. For comparison, typical ranges of magnetic moments of these cations in several oxidation states (*13*) are also given. In agreement with previous flow microbalance experiments (*1-3*), these results shown that Cr, Fe, and Cu cations undergo redox during treatments with H_2 and O_2. The magnetic moments suggest that most of the Cr in Cr-Y is Cr(III) after reduction with H_2, and Cr(V) after oxidation with O_2. For Cu-Y,

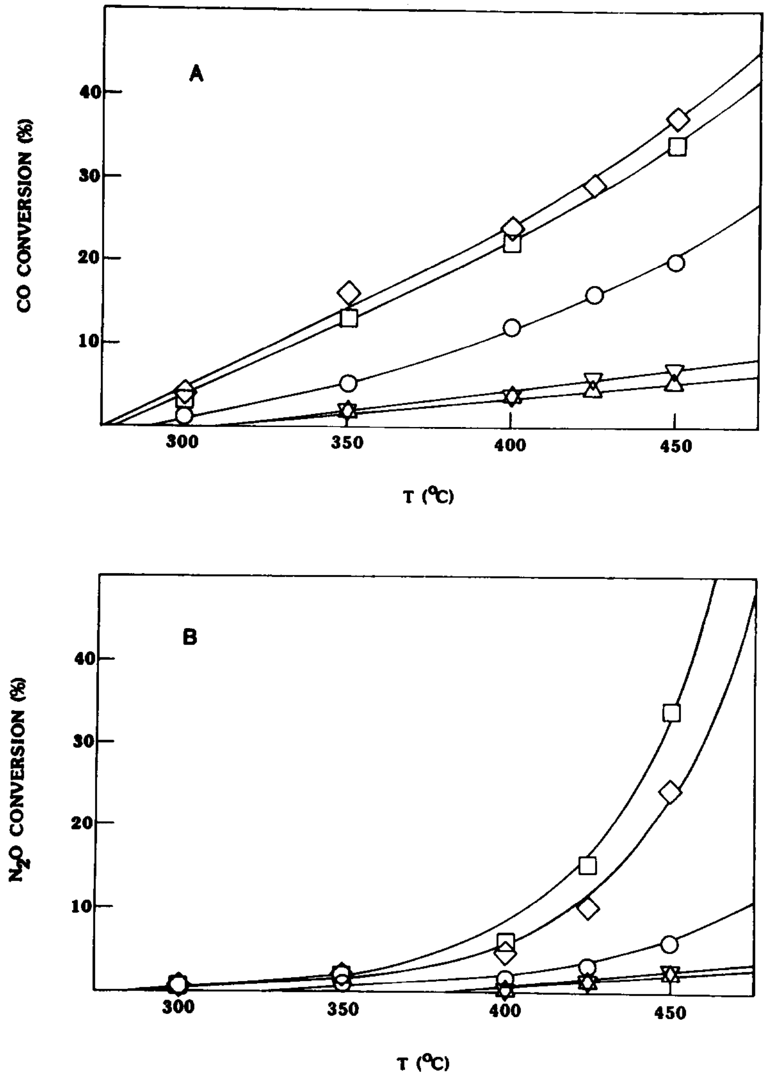

FIG. 4. CO conversions (A) and N_2O conversions (B) of FeLa–Y (◇), FeEu–Y (□), Fe–Y (○), La–Y (▽), and Eu–Y (△).

the magnetic moments suggest an oxidation state of Cu(II) after oxidation, and partial reduction to Cu(I) after reduction. In the previous microbalance experiments, complete reduction to Cu(I) was not achieved until the Cu–Y had undergone several repeated redox cycles (*3*). For Fe–Y, it is known from Mössbauer spectroscopy that the oxidation state of Fe is Fe(III) after treatment with O_2, and Fe(II) after treatment with H_2. The magnetic moment was found to be in the range for Fe(II) after the reduction treatment, in agreement with the Mössbauer spectroscopy results. However, after the oxidation treatment the measured magnetic moment was 4.4 μ_B, a value too low for Fe(III). This low value is indicative of ferric cations that are not magnetically dilute, suggesting that an antiferromagnetic interaction takes place between Fe(III) cations. The reason for this behavior could be that Fe cations became paired during the oxidation process, perhaps forming Fe–O–Fe bridges (*11*). The two Fe cations of such

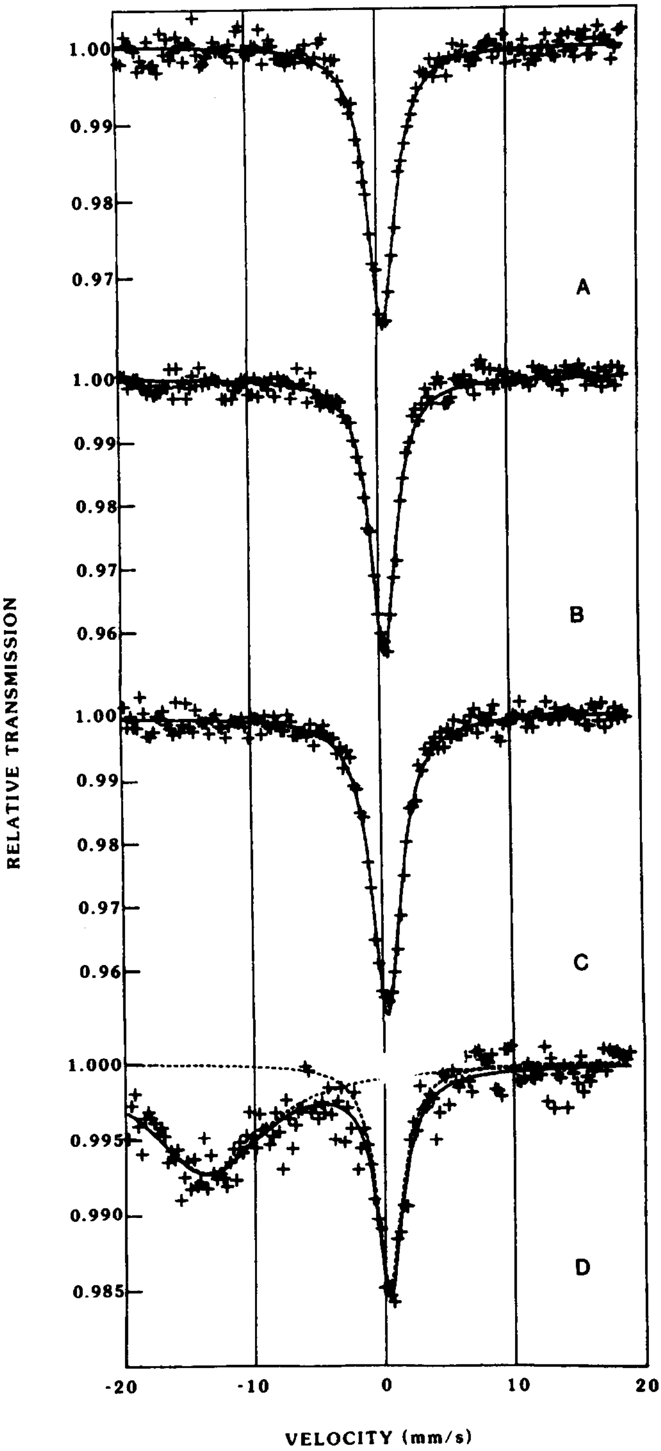

FIG. 5. Room temperature europium-151 Mössbauer spectra. (A) Eu–Y after oxidation pretreatment, (B) Eu–Y after reduction pretreatment, (C) FeEu–Y after oxidation pretreatment, (D) FeEu–Y after reduction pretreatment.

TABLE 2

Mössbauer Spectroscopy Parameters of FeCa–Y, FeLa–Y, FeEu–Y, and Eu–Y

Sample	^{57}Iron spectra: After oxidation					
	Fe^{3+} outer doublet			Fe^{3+} inner doublet		
	I.S. (mm/s)	Q.S. (mm/s)	Area (% mm/s)	I.S. (mm/s)	Q.S. (mm/s)	Area (% mm/s)
FeCa–Y	0.38	1.86	1.76	0.37	1.10	0.74
FeLa–Y	0.37	1.88	0.89	0.39	1.08	0.72
FeEu–Y	0.38	1.85	2.56	0.35	1.10	0.71
	After reduction					
	Fe^{2+} outer doublet			Fe^{2+} inner doublet		
FeCa–Y	1.11	2.28	1.43	0.91	0.64	0.90
FeLa–Y	1.17	2.32	0.85	0.92	0.61	1.11
FeEu–Y	1.15	2.36	1.15	0.92	0.61	2.00
	^{151}Europium spectra: After oxidation					
	Eu^{3+}			Eu^{2+}		
Eu–Y	0.40		14.8	—		—
FeEu–Y	0.36		20.2	—		—
	After reduction					
	Eu^{3+}			Eu^{2+}		
Eu–Y	0.41		16.3	—		—
FeEu–Y	0.36		5.5	−13.8		12.2

a bridge would be in sufficiently close proximity for an antiferromagnetic interaction to occur.

The magnetic moments of Mn, Co, and Ni showed that these cations remained in their divalent state after either oxidizing or reducing treatment. This agrees with previous flow microbalance experiments performed on Mn–Y (*1*). It also agrees with temperature-programmed oxygen desorption results, in which an oxygen signal was detected for oxygen-treated Cr–Y, Fe–Y, and Cu–Y, but not for Co–Y and Ni–Y (*14*). However, a recent flow microbalance experiment on Co–Y revealed that oxygen treatment may oxidize a small fraction of the Co to Co(III) (*15*). The magnetic susceptibility experiments are not sufficiently sensitive to detect changes in the oxidation state of a small fraction of the cations.

Figure 6 shows CO and N_2O conversions versus temperature over these singly exchanged zeolites under identical experimental conditions. To calculate turnover frequencies, these data were corrected to a standard set of reaction pressures by assuming rate laws of the form $r = kP_{NO}$ for the oxidation of CO with NO over Fe–Y and Cu–Y, and of the form $r = kP_{N_2O}$ for the decomposition of N_2O over Fe–Y, Co–Y, and Cu–Y. These are the rate laws determined previously for Fe–Y (*2, 4*). The above rate law for the oxidation of CO was extended to Cu–Y because this catalyst tends to remain in its reduced state when CO is present, even in the presence of ex-

TABLE 3

Magnetic Moments of First-Row Transition Metal Cations

Sample	Treatment	Magnetic moment (μ_B)	Typical values (μ_B)
Cr–Y	O_2, 700 K	1.9	Cr(IV) : 2.7–2.8, Cr(V) : 1.7–1.8, Cr(VI) : 0.4–0.9
Cr–Y	H_2, 700 K	4.1	Cr(II) : 4.8–5.1, Cr(III) : 3.6–4.0
Mn–Y	O_2, 700 K	5.7	Mn(II) : 5.1–5.9
Mn–Y	H_2, 700 K	5.7	Mn(II) : 5.1–5.9
Fe–Y	O_2, 700 K	4.4	Fe(III) : 5.6–6.0
Fe–Y	H_2, 700 K	4.6	Fe(II) : 4.6–5.9
Co–Y	O_2, 700 K	4.8	Co(II) : 4.2–5.4
Co–Y	H_2, 700 K	4.8	Co(II) : 4.2–5.4
Ni–Y	O_2, 700 K	4.0	Ni(II) : 2.9–4.0
Ni–Y	H_2, 700 K	4.0	Ni(II) : 2.9–4.0
Cu–Y	O_2, 700 K	2.1	Cu(II) : 1.6–2.9
Cu–Y	H_2, 700 K	0.6	Cu(I) : 0.0, Cu(II) : 1.6–2.9

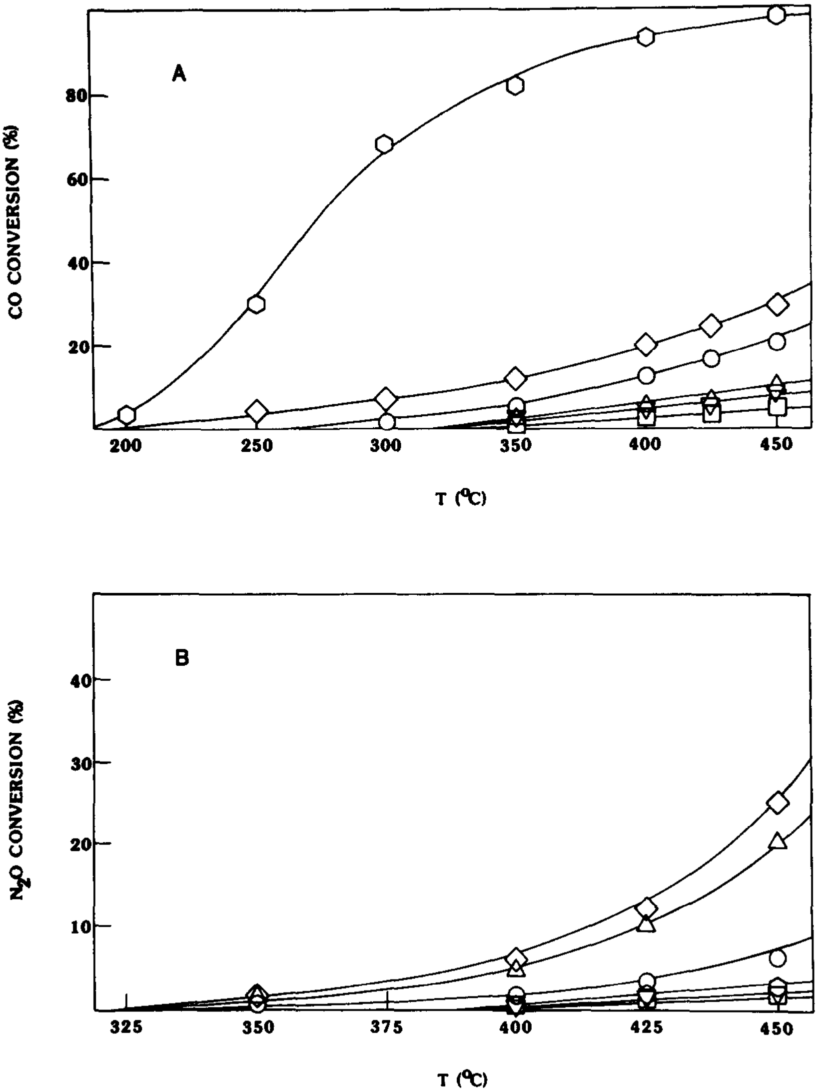

FIG. 6. CO conversions (A) and N_2O conversions (B) of Cr–Y (⬡), Mn–Y (□), Fe–Y (○), Co–Y (△), Ni–Y (▽), and Cu–Y (◇).

cess O_2 (a better oxidizing agent than NO) (*3*). The above rate law for the decomposition of N_2O was extended to Co–Y and Cu–Y because N_2O is the only reactant; thus, the rate law should be the same regardless of whether the oxidation step or the reduction step is rate limiting. In all of the above cases, the corrections to the turnover frequencies were at most 25%. For the calculation of turnover frequencies for the oxidation of CO with NO over Cr–Y, a more detailed kinetic study was performed (due to the high activity of this catalyst). This study revealed a rate law of the form $r = kP_{CO}$ and an apparent activation energy of 57 kJ/mol. For the remaining zeolites, rate laws were not needed, since conversions were low and effluent partial pressures did not differ much from inlet partial pressures. Turnover frequencies at 720 K obtained in this manner are listed in Table 4.

The results summarized in Fig. 6 and Ta-

TABLE 4

Turnover Frequencies of First-Row Transition Metal Cations

$CO + NO \rightarrow CO_2 + N_2$[a]		$2N_2O \rightarrow 2N_2 + O_2$[b]	
Sample	Turnover frequency (mol CO/mol cation · s)	Sample	Turnover frequency (mol N_2O/mol cation · s)
Cr–Y	4.2×10^{-2}	Cr–Y	1.1×10^{-4}
Mn–Y	1.3×10^{-4}	Mn–Y	6.4×10^{-5}
Fe–Y	7.7×10^{-4}	Fe–Y	4.6×10^{-4}
Co–Y	3.0×10^{-4}	Co–Y	1.7×10^{-3}
Ni–Y	2.7×10^{-4}	Ni–Y	7.4×10^{-5}
Cu–Y	8.3×10^{-4}	Cu–Y	1.7×10^{-3}

[a] Reaction conditions: temperature, 720 K; gas composition, 3% CO, 6% NO, balance He; total flow rate, 200 cm^3 (STP)/min.

[b] Reaction conditions: temperature, 720 K; gas composition, 8% N_2O, balance He; total flow rate, 200 cm^3 (STP)/min.

ble 4 show that Mn–Y and Ni–Y are relatively inactive for both reactions. Iron and copper Y-zeolites display a moderate activity for both reactions, with Cu–Y being more active than Fe–Y for the decomposition of N_2O. The most interesting results are those obtained for Cr–Y and Co–Y. Chromium Y-zeolite was found to be considerably more active than either Fe–Y or Cu–Y for the oxidation of CO with NO. However, the same zeolite exhibited no activity for the decomposition of N_2O. In contrast, Co–Y had only a limited activity for the oxidation of CO with NO, but was as active as Cu–Y for the decomposition of N_2O. Such results show that a transition metal-exchanged zeolite that is active for one redox reaction may not necessarily be active for another redox reaction.

FeCr–Y, FeMn–Y, FeCo–Y, FeNi–Y, and FeCu–Y

Figure 7 shows ^{57}Fe Mössbauer spectra of these coexchanged samples after treatment with O_2 at 700 K. WIth the exception of FeCr–Y, the spectra are similar to those obtained for Fe–Y after the same pretreatment (*6, 11*), showing a broad Fe(III) doublet. The FeCr–Y sample, in addition to this doublet, has an extra Fe(III) doublet with an unusually large quadrupole splitting (2.7 mm/s). Such a doublet is indicative of Fe(III) cations in sites of low symmetry. Since Fe–Y has been found to take up one oxygen atom for every two Fe cations upon oxidation (*2, 11*), suggesting that oxygen adsorbs on pairs of cations, it could be postulated that this doublet is due to Fe cations that became paired with Cr cations during the oxidation process. However, since evidence of collapse of the lattice was seen in the chemical analysis of this sample, it could also be postulated that this doublet is due to Fe cations associated with an amorphous chromium oxide species.

After treatment with H_2 at 700 K, the zeolite samples gave the Mössbauer spectra shown in Fig. 8. With the exception of FeCu–Y, all samples gave spectra where the outer doublet dominated the total spectral area. This can be interpreted as meaning that in all these zeolite except FeCu–Y, most Fe cations are located in site I. Thus, of all these cations, only Cu has a sufficiently strong preference for site I that it tends to not be displaced from that site during exchange with Fe. The parameters obtained by computer-fitting the spectra of Figs. 7 and 8 are summarized in Table 5.

Figures 9 and 10 show CO and N_2O conversions versus temperature measured for these zeolites. For comparison, conver-

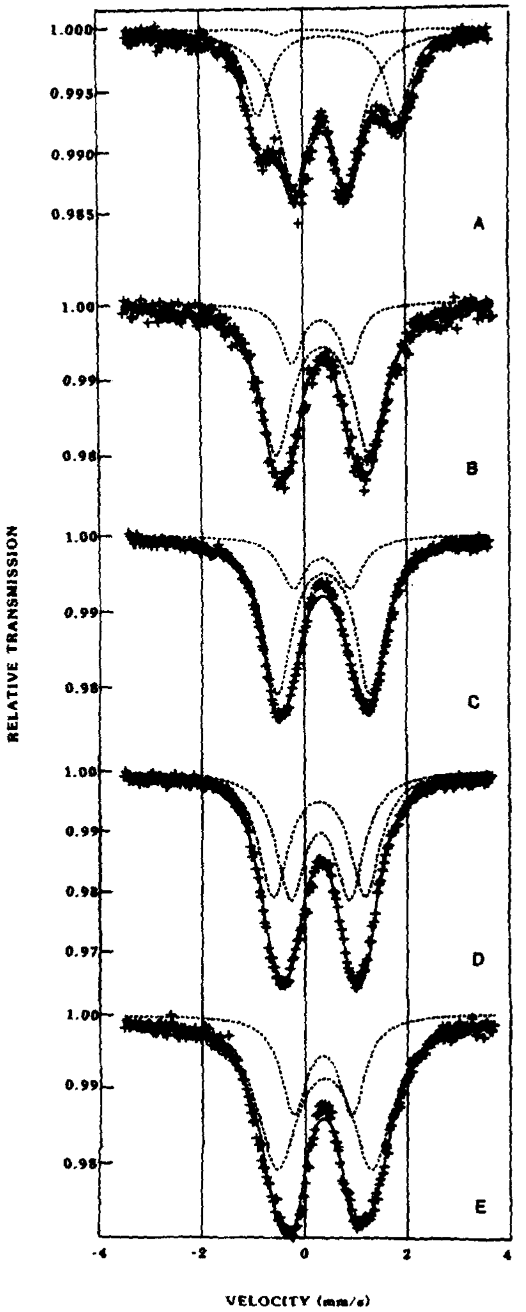

FIG. 7. Room temperature iron-57 Mössbauer spectra of (A) FeCr–Y, (B) FeMn–Y, (C) FeCo–Y, (D) FeNi–Y, and (E) FeCu–Y after oxidation pretreatment.

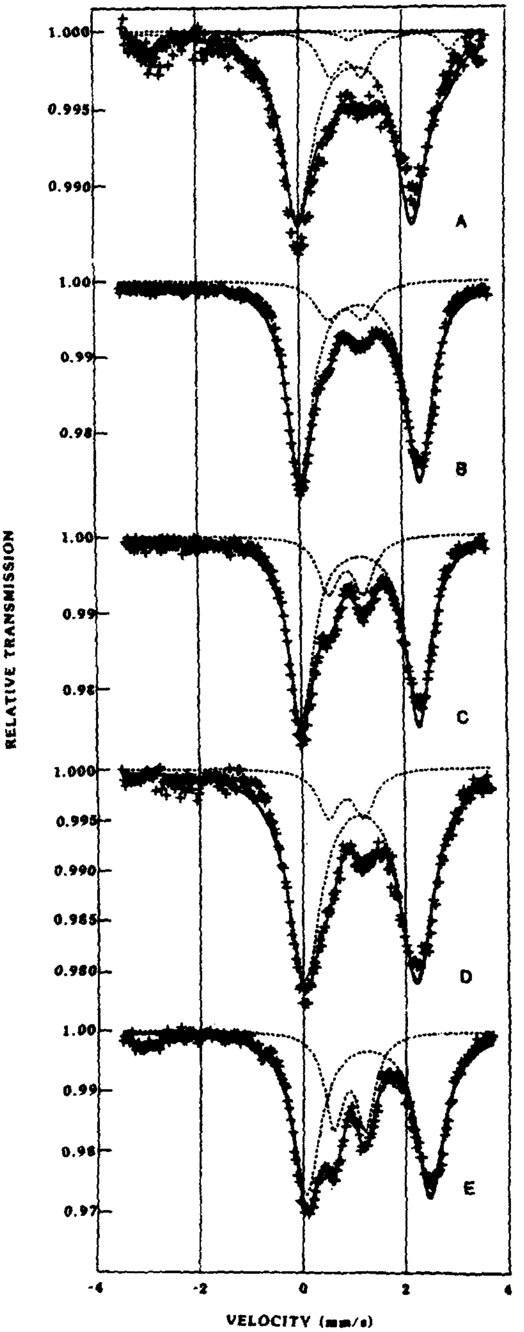

FIG. 8. Room temperature iron-57 Mössbauer spectra of (A) FeCr–Y, (B) FeMn–Y, (C) FeCo–Y, (D) FeNi–Y, and (E) FeCu–Y after reduction pretreatment.

sions calculated from the cation loadings of these samples and the turnover frequencies of Table 4 are also shown. For FeCr–Y and FeCo–Y, the observed conversions matched the predicted conversions within experimental error. In the other zeolites, a

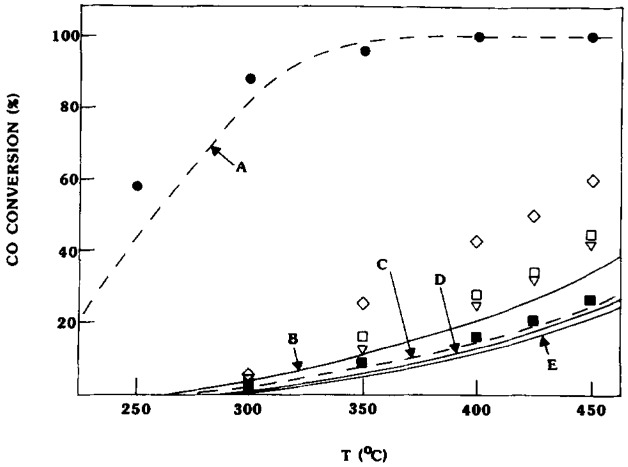

FIG. 9. Calculated and measured CO conversions for coexchanged zeolites. (●) FeCr–Y, (◇) FeCu–Y, (□) FeMn–Y, (▽) FeNi–Y, (■) FeCo–Y. Curve A was calculated for FeCr–Y, curve B for FeCu–Y, curve C for FeCo–Y, curve D for FeNi–Y, and curve E for FeMn–Y.

synergistic effect was observed. The measured conversions for the oxidation of CO with NO were higher than expected, while the measured conversions for the decomposition of N_2O were lower than expected. Given that the rate-determining step for N_2O decomposition over Fe–Y is believed to be the reduction of the catalyst while the slow step in the oxidation of CO by NO is believed to be the oxidation of the catalyst, the results of this study suggest that the presence of coexchanged Mn and Ni increases the oxidizability of Fe while decreasing its reducibility. In FeCu–Y, although it is not clear which cations catalyze the reactions, a similar effect occurs.

DISCUSSION

Effect of Coexchanged Polyvalent Cations on Fe Cation Location

Polyvalent cations exchanged into Y-zeolite are known to have a stronger preference for site I than monovalent cations. For example, X-ray diffraction studies of Ca–Y and La–Y have shown that these cations tend to migrate to site I when they lose their extralattice ligands (*16–18*). Similar observations have been made for Cu and Co cat-

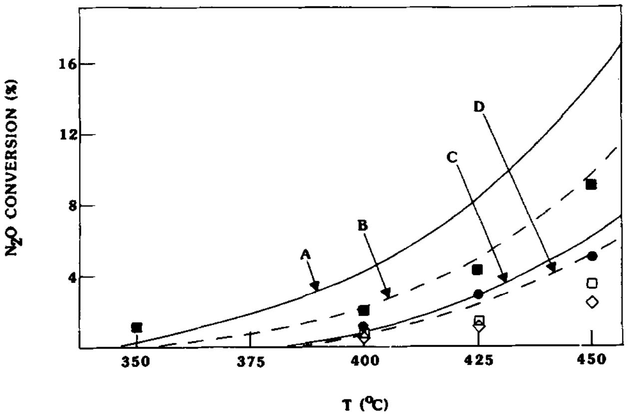

FIG. 10. Calculated and measured N_2O conversions for coexchanged zeolites. (■) FeCo–Y, (●) FeCr–Y, (□) FeMn–Y and FeNi–Y, (◇) FeCu–Y. Curve A was calculated for FeCu–Y, curve B for FeCo–Y, curve C for FeMn–Y and FeNi–Y, and curve D for FeCr–Y.

TABLE 5

Mössbauer Spectroscopy Parameters of FeCr–Y, FeMn–Y, FeCo–Y, FeNi–Y, and FeCu–Y

Sample	After oxidation								
	Fe^{3+} outer doublet			Fe^{3+} inner doublet			Fe/chromium oxide		
	I.S. (mm/s)	Q.S. (mm/s)	Area (% mm/s)	I.S. (mm/s)	Q.S. (mm/s)	Area (% mm/s)	I.S. (mm/s)	Q.S. (mm/s)	Area (% mm/s)
FeCr–Y	0.39	1.81	0.10	0.35	1.05	2.63	0.50	2.73	1.21
FeMn–Y	0.38	1.82	4.64	0.35	1.14	1.13	—	—	—
FeCo–Y	0.38	1.83	4.37	0.34	1.11	1.25	—	—	—
FeNi–Y	0.29	1.80	4.44	0.31	1.15	4.30	—	—	—
FeCu–Y	0.39	1.86	6.07	0.35	1.14	2.40	—	—	—
	After reduction								
	Fe^{2+} outer doublet			Fe^{2+} inner doublet				Metallic Fe	
FeCr–Y	1.10	2.24	2.72	0.92	0.61	0.39		0.20	
FeMn–Y	1.18	2.33	4.93	0.91	0.69	0.84		0	
FeCo–Y	1.15	2.30	4.48	0.89	0.68	1.08		0	
FeNi–Y	1.13	2.19	5.03	0.86	0.69	0.72		0	
FeCu–Y	1.27	2.41	5.33	0.90	0.61	2.04		0	

ions (*10, 19, 20*). In addition, a theoretical study in which the bonding between the cations and the framework structure was assumed to be ionic concluded that divalent cations should have a strong preference for site I over site II while the site preferences of monovalent cations should depend on the cationic radii (*21, 22*).

In this study, La, Eu, Ca, and Cu were found to have a sufficiently strong preference for site I to force substantial amounts of Fe to sites I′, II, and/or II′. The effect was more pronounced with La and Eu than with Ca and Cu, suggesting that larger cations have a stronger preference for site I because of the long cation–oxygen bonds of that site. The same effect was not observed when Cr, Mn, Co, or Ni cations were coexchanged with Fe. Since cations tend to migrate to site I only after losing all extralattice ligands, this may be an indication that Cr, Mn, Co, and Ni cations do not lose their extralattice ligands as easily as Fe and Cu. It must also be noted that the loadings of Mn, Co, and Ni in FeMn–Y, FeCo–Y, and FeNi–Y were relatively low. Thus, it is possible that these cations would force iron to sites other than site I at higher loadings. In fact, a recent Mössbauer spectroscopic study of an FeCo–Y sample prepared by coexchanging Fe and Co simultaneously showed that the iron in the sample contributed predominantly an Fe^{2+} inner doublet to the spectrum, indicating that a large fraction of the Fe was in sites I′, II, and/or II′ (*23*).

Effects of Coexchanged Cations on Oxidizabilities and Reducibilities

The results summarized above revealed several cases where the presence of one cation affected the redox properties of another coexchanged cation. For instance, the ^{151}Eu Mössbauer spectra showed that the presence of Fe enhances the reducibility of Eu(III) to Eu(II). In a similar way, the measured reaction rates over FeMn–Y and FeNi–Y showed that Mn and Ni enhance the oxidizability of Fe(II) to Fe(III). Reaction rates over FeCu–Y also showed that one of these cations enhances the oxidizability of the other. Effects similar to these have been reported before for FeRu–Y by Good *et al.* (*24*). They found that the presence of Fe in this zeolite inhibits the reducibility of Ru to the metal, while Ru enhances the reducibility of Fe to Fe(II).

The changes in the redox properties of iron brought about by coexchanged cations could be explained by the formation of cation–oxygen–cation bridges involving two different types of cations. Garten *et al.* proposed the existence of Fe–O–Fe bridges in oxidized Fe–Y to account for the oxygen carrying capacity of that zeolite (*11*). In the coexchanged zeolites of this study, it is possible that Fe–O–Mn, Fe–O–Ni, Fe–O–Cu, and Fe–O–Eu bridges are formed. The thermodynamic properties of bridges involving two types of cations could differ from those of bridges involving only one type of cation, explaining the observed changes in the redox properties. Evidence suggesting the existence of La–O–Ni bridges was found in a previous study of LaNi–X (*25*).

The Fe–O–Fe bridges proposed in the previous work on Fe–Y were formed upon oxidation of Fe(II) to Fe(III). Since cations such as Mn and Ni are not believed to undergo changes in their oxidation states, bridges involving these cations are probably formed through a different mechanism. One possibility is that they form from Fe–O–Fe bridges as shown below:

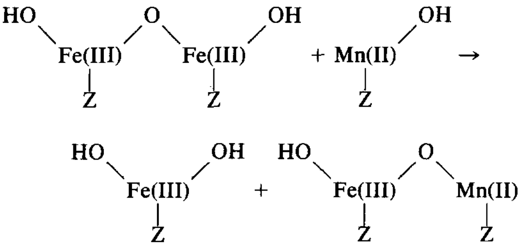

The driving force for such a reaction could be that the oxygen in an OH^- group is a stronger Lewis base than the oxygen in a cation–oxygen–cation bridge. It is known from solution chemistry that OH^- is a stronger base than ions such as $HCrO_4^-$ and MnO_4^- where oxygen is bonded to a first-row transition metal (*26*). Since Fe(III) would be expected to be a stronger Lewis acid than Mn(II), Ni(II), Cu(II), or Eu(III) because of its higher charge/size ratio, a strong base like OH^- would bond preferentially to Fe(III).

It should be mentioned that, although in this work treatment with H_2 did not reduce the Eu in Eu–Y to the divalent state, other authors have reported the reduction of Eu to Eu(II) in the same zeolite. However, the lengths of the reduction treatments in these cases may have been longer, and the extents of reductions may not have been high. Samuel and Delgass reported that most of the Eu in Eu–Y could be reduced to Eu(II) by treatment at 720 K with H_2, but they did not report the length of the treatment (*27*). In agreement with their results, the Eu(II) Mössbauer spectroscopy peak observed in the present study for FeEu–Y was quite broad, showing that their sample and the samples of this study were not very different. Stucky *et al.* (*28*) reported a Eu(II) EPR band after degassing Eu–Y at 600 K, but they did not measure the extent of Eu reduction. Arakawa *et al.* (*29*) reported that Eu in Eu–Y could be reduced by outgassing at 870 K for 2 h, but from magnetic susceptibility measurements they concluded that only 0.1% of the Eu had been reduced.

Differences between Various First-Row Transition Metals

Magnetic moments of first-row transition metals exchanged into zeolites have been studied before by various investigators (*10, 30, 31*); however, the present study is the first in which the technique was used to systematically study the oxidation states of several metals after oxidizing and reducing pretreatments. When a comparison is made between the measured magnetic moments and the measured reaction rates, it is seen that metals that do not undergo oxidation and reduction (i.e., Mn and Ni) are inactive for the type of redox reactions of this study.

Metals that undergo redox during treatment with H_2 and O_2 (i.e., Cr, Fe, and Cu) are active for at least one of these reactions. The only exception may be Co–Y. Preliminary microbalance studies have shown that a small fraction of the Co may be oxidized to Co(III) by treatment with O_2 (*15*); however, this was not detected in the magnetic susceptibility experiments. This zeolite was found to be active for the decomposition of N_2O, but not for the oxidation of CO with NO. Such results contribute further evidence supporting the regenerative redox mechanism previously proposed for these reactions.

As was mentioned above, the rate-determining step for the oxidation of CO with NO over Fe–Y has been found to be the oxidation of the catalyst. The rate-determining step for the decomposition of N_2O over the same catalyst has been found to be the reduction of the catalyst. Hence, the fact that Cr–Y is active for the oxidation of CO with NO but not for the decomposition of N_2O is an indication that Cr cations are easily oxidized but not easily reduced. In fact, Cr cations seem to be so easily oxidized that, in contrast to Fe–Y, chromium Y-zeolite operates in its oxidized state when catalyzing the oxidation of CO with NO. Since Co–Y behaves in an opposite manner, the reaction rates over this zeolite indicate that Co cations are easily reduced to Co(II), but not easily oxidized to Co(III). This would agree with the magnetic moment measured for Co–Y. Since Fe–Y and Cu–Y catalyze both reactions, it can be assumed that their redox properties lie somewhere between those of Cr and Co. Hence, the data show that the oxidizabilities of these cations decrease in the order Cr(III) > Fe(II), Cu(I) > Co(II) > Mn(II), Ni(II).

These results agree with oxidizabilities calculated for divalent transition metal ions in zeolites using ligand field theory by Klier *et al.* (*32*). These authors calculated that the oxidizabilities of first-row divalent transition metals decrease with increasing atomic number, with the oxidizability of Mn(II) being lower than expected, and that of Fe(II) being higher than expected because of the stability of the half-filled 3*d* shell of Mn(II) and Fe(III). Hence, it is conceivable that the oxidizabilities of divalent cations decrease in the order Cr(II) > Fe(II) > Co(II) > Mn(II) > Ni(II) > Cu(II). The oxidizabilities of Mn(II) and Ni(II) would be too low for these cations to undergo redox, while the cations Cr(II), Fe(II), and Co(II) could catalyze the reactions by being oxidized to higher oxidation states. Copper Y-zeolites would be able to act as a catalyst because Cu(II) can be reduced to Cu(I).

The measured oxidizabilities could also be predicted by a simpler model which takes into account only the ionization energies of the cations and their coordination numbers. In this model, the bond energy of a cation–oxygen bond was assumed to be proportional to the oxidation state of the cation. The value of the energy of formation of a cation–oxygen single bond from O^{2-} and the corresponding cation was taken to be 970 kJ/mol times the oxidation state of the cation. This value was derived from the average heat of formation of diatomic molecules involving oxygen and a first-row transition metal (*33*). To arrive at the value, it was assumed that the oxidation state of the cations in the diatomic molecules was 2+, that they formed double bonds with oxygen, and that the energy of a double bond was equal to 1.75 times the energy of a single bond. In the zeolite, the cations were assumed to be singly bonded to three oxygens in their lower oxidation states (as they would be in sites I′, II, and II′), and to four oxygens (three from the lattice and one extralattice) in their higher oxidation states. In the case of Cr–Y, the oxidation state of Cr was assumed to change from 3+ to 5+, so the bond between Cr(V) and the extralattice oxygen was assumed to be a double bond instead of a single bond. The oxidizabilities calculated from ionization energies and assumed bond energies decreased in the order Cr(III) > Cu(I) > Fe(II) > Co(II)

> Mn(II) > Ni(II), in agreement with the experimental results. In a manner similar to that described here, catalytic activities of zeolite exchanged with first-row transition metals for the oxidation of CO with O_2 were correlated with ionization energies in a previous study by Kubo *et al.* (*34*).

Although the Cr–Y and FeCr–Y samples of this study were found to be quite active for the oxidation of CO with NO, care must be taken in the interpretation of these results. Evidence was found by chemical analysis that a portion of the zeolite lattice collapsed during Cr exchange. Thus, some of the activity in these samples may have come from an amorphous chromium oxide species.

Oxidation Process in Fe–Y and Cu–Y

When Fe–Y and Cu–Y are oxidized, it is found that these zeolites take up an amount of oxygen corresponding to one oxygen atom for every two cations (*1–3*). This implies that pairs of cations must come together for the oxidation process to occur. For Fe–Y, two models have been proposed to describe its oxygen carrying capacity. In one model, it was suggested that Fe–O–Fe bridges formed upon oxidation (*11*), whereas in a later model it was proposed that a single Fe(III) cation in site III′ could hold an oxygen atom, with one electron being supplied by a second Fe cation (*35*). Regardless of which model is adopted, pairs of Fe cations must migrate to some degree of proximity for oxidation to occur. The magnetic susceptibility results summarized above indicate that the distance between Fe cations in oxidized Fe–Y is sufficiently small that antiferromagnetic effects are detected. For Cu–Y, the same effect may not have been detectable because of the wider range of typical magnetic moments of Cu(II) than that of Fe(III).

ACKNOWLEDGMENTS

The authors express their gratitude to the National Science Foundation for Grant CBT-8414622 which supported this work. We also thank Professor W. K. Hall for valuable advice during this project.

REFERENCES

1. Fu, C. M., Deeba, M., and Hall, W. K., *Ind. Eng. Chem. Prod. Res. Dev.* **19,** 229 (1980).
2. Petunchi, J. O., and Hall, W. K., *J. Catal.* **78,** 327 (1982).
3. Petunchi, J. O., and Hall, W. K., *J. Catal.* **80,** 403 (1983).
4. Fu, C. M., Korchak, V. N., and Hall, W. K., *J. Catal.* **68,** 166 (1981).
5. Leglise, J., Petunchi, J. O., and Hall, W. K., *J. Catal.* **86,** 392 (1984).
6. Aparicio, L. M., Dumesic, J. A., Fang, S. M., Long, M. A., Ulla, M. A., Millman, W. S., and Hall, W. K., *J. Catal.* **104,** 381 (1987).
7. Aparicio, L. M., Hall, W. K., Fang, S. M., Ulla, M. A., Millman, W. S., and Dumesic, J. A., submitted for publication.
8. Garwood, W. E., Lucki, S. J., Chen, N. Y., and Bailar, J. C., Jr., *Inorg. Chem.* **17,** 610 (1978).
9. Miró, E. E., Ardiles, D. R., Lombardo, E. A., and Petunchi, J. O., *J. Catal.* **97,** 43 (1986).
10. Egerton, T. A., Hagan, A., Stone, F. S., and Vickerman, J. C., *J. Chem. Soc. Faraday Trans. 1* **68,** 723 (1972).
11. Garten, R. L., Delgass, W. N., and Boudart, M., *J. Catal.* **18,** 90 (1970).
12. Delgass, W. N., Garten, R. L., and Boudart, M., *J. Phys. Chem.* **73,** 2970 (1969).
13. Figgis, B. N., and Lewis, J., *Prog. Inorg. Chem.* **6,** 37 (1964).
14. Iwamoto, M., Nakamura, M., Nagano, H., Kagawa, S., and Selyama, T., *J. Phys. Chem.* **86,** 153 (1982).
15. Millman, W. S., and Hall, W. K., private communication.
16. Costenoble, M. L., Mortier, W. J., and Uytterhoeven, J. B., *J. Chem. Soc. Faraday Trans. 1* **74,** 466 (1978).
17. Bennett, J. M., and Smith, J. V., *Mater. Res. Bull.* **3,** 633 (1968).
18. Bennett, J. M., and Smith, J. V., *Mater. Res. Bull.* **3,** 865 (1968).
19. Ichikawa, T., and Kevan, L., *J. Phys. Chem.* **87,** 4433 (1983).
20. Gallezot, P., and Imelik, B., *J. Chim. Phys.* **71,** 155 (1974).
21. Dempsey, E., *in* "Molecular Sieves," p. 293. Society of Chemical Industry, London, 1968.
22. Dempsey, E., *J. Phys. Chem.* **73,** 3660 (1969).
23. Lin, T. A., Schwartz, L. H., and Butt, J. B., *J. Catal.* **97,** 177 (1986).
24. Good, M. L., Akbarnejad, M., and Donner, J., "Symp. Metal Clusters in Catal.," p. 763. Amer. Chem. Soc., Div. Petrol. Chem., Washington, DC, 1980.
25. Briend-Faure, M., JeanJean, J., Spector, G., Delafosse, D., and Bozon-Verduraz, F., *J. Chim. Phys.* **79,** 489 (1982).

26. Dean, J. A. (Ed.), "Lange's Handbook of Chemistry." McGraw–Hill, New York, 1985.

27. Samuel, E. A., and Delgass, W. N., *J. Chem. Phys.* **62,** 1590 (1975).

28. Stucky, G. D., Iton, L., Morrison, T., Shenoy, G., Suib, S., and Zerger, R., *J. Mol. Catal.* **27,** 71 (1984).

29. Arakawa, T., Takata, T., Takakuwa, M., Adachi, G., and Shiokawa, J., *Mater. Res. Bull.* **17,** 171 (1982).

30. Rubinstejn, A. M., Slinkin, A. A., Loktev, M. I., Fedorovskaja, E. A., Bremer, H., and Vogt, F., *Z. Anorg. Allg. Chem.* **423,** 164 (1976).

31. Bremer, H., Schödel, R., Vogt, F., Rubinstejn, A. M., Slinkin, A. A., and Fedorovskaja, G. A., *Z. Chem.* **13,** 350 (1973).

32. Klier, K., Hutta, P. J., and Kellerman, R., *Amer. Chem. Soc. Symp. Ser.* **40,** 108 (1977).

33. Weast, R. C. (Ed.), "CRC Handbook of Chemistry and Physics." CRC Press, Boca Raton, FL, 1982.

34. Kubo, T., Tominaga, H., and Kunugi, T., *Bull. Chem. Soc. Japan* **46,** 3549 (1973).

35. Segawa, K., Chen, Y., Kubsh, J. E., Delgass, W. N., Dumesic, J. A., and Hall, W. K., *J. Catal.* **76,** 112 (1982).